

Dynamical Breaking of Charge Neutrality in Intrinsic Josephson Junctions: Common Origin for Microwave Resonant Absorptions and Multiple-branch Structures in the I-V Characteristics

^a M. Machida

*Center for Promotion of Computational Science and Engineering,
Japan Atomic Energy Research Institute, 2-2-54 Nakameguro, Meguro-ku Tokyo 153, Japan
^a CREST, Japan Science and Technology Corporation (JST), Japan*

T.Koyama

Institute for Materials Research, Tohoku University, Katahira 2-1-1, Aoba-ku, Sendai 980-77, Japan

M.Tachiki

*National Research Institute for Metals, Sengen 1-2-1, Tsukuba, Ibaraki 305, Japan
(September 17, 2018)*

We demonstrate that both microwave resonant absorptions and multiple-branch structures in the I-V characteristics observed in intrinsic Josephson junctions (IJJ's) are caused by dynamical breaking of charge neutrality (DBCN) inside the atomic-scale superconducting layer. The Lagrangian for the time-dependent Lawrence-Doniach model incorporating the effect of the DBCN is proposed, and the longitudinal collective Josephson plasma mode is proved to exist based on the Lagrangian. On the other hands, the branching behaviors in the I-V curves are almost completely reproduced by careful numerical simulations for the model equation derived from the Lagrangian.

PACS numbers: 74.25.Fy, 74.50.+r, 74.80.Dm

Intrinsic Josephson effects (IJE's) in highly anisotropic high temperature superconductors (HTSC's) have attracted growing interests [1], [2], and recent extensive experimental studies have discovered two remarkable phenomena for IJE's, i.e., the microwave resonant absorptions (MRA's) [3] and the multiple-branch structures (MBS's) in I-V characteristics along the c-axis [4].

In Bi-2212 single crystals(SC's), the MRA has been observed for both longitudinal and transverse microwave configurations in cavities, and the observed dispersion relations have clearly been distinguished from one another for those configurations [5]. The MRA in the longitudinal configuration is caused by the excitation of the longitudinal Josephson plasma mode propagating along the c-axis, and the existence of such the charge fluctuation mode indicates that the charge neutrality can be dynamically broken inside the superconducting layer under the application of an AC electric field along the c-axis. Thus, a novel coupling between junctions due to the DBCN has been suggested and new collective dynamical behaviors have been expected to emerge [6], [7].

On the other hands, the I-V curves along the c-axis in Bi-2212 SC's are composed of many branches with almost equal inter-branch spacing and the number of those is equal to the number of junctions [4], [8]. It has been widely believed that such structures manifests the independence of junctions inside IJJ's, that is, the coupling between junctions is negligible, and then, each junction behaves independently [8]. Thus, such a understanding for the I-V curves is irreconcilable with the above in-

terpretation for the MRA experiments, and the understanding for IJE's is now still controversial for the two experimental results.

In this paper, we explain the DBCN inside the superconducting layer in IJJ's, and give a proper model Lagrangian for IJJ's. By using the Lagrangian we prove that the c-axis propagating longitudinal plasma mode exists, and show that the MBS in the I-V characteristics can be well reproduced by careful numerical simulations for the model equation derived from the Lagrangian [7], [9]. Thus, we clarify that both the MRA and the MBS have the common origin, i.e., the DBCN.

Now, let us explain about the DBCN in IJJ's. Figure.1(a) and (b), respectively, are a schematic figure for physical events followed by the electron tunneling in conventional stacked SIS junction (CSISJ) system and IJJ. From the figures, it is found that the charges are confined near the surface in the CSISJ system while the whole of the superconducting layer is charged in the IJJ, i.e., the DBCN occurs. This is because the superconducting CuO₂ layer in IJJ's is extremely thin ($\sim 3\text{\AA}$), i.e., the thickness is comparable to the charge screening length and therefore the charge screening becomes incomplete within the single superconducting layer. In CSISJ systems, the electric field generated at a junction site is completely screened out by sufficiently thick superconducting layers, and the coupling between different junction-sites is not formed. On the other hands, in IJJ's, the electric field generated inside a junction site affects the neighboring junction sites and therefore the coupling between

junctions emerges [7], [9].

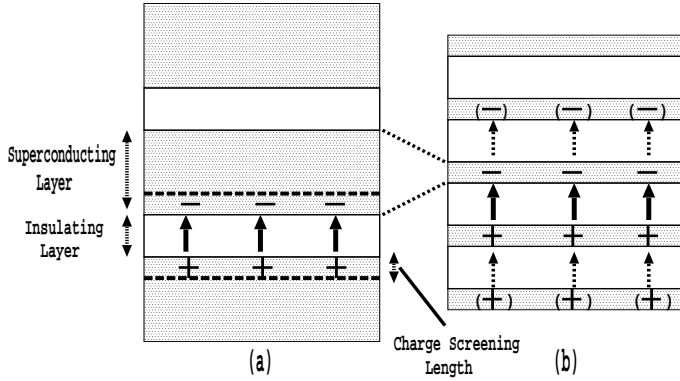


FIG.1 Schematic views of (a) the conventional stacked SIS junction (CSISJ) and (b) the intrinsic Josephson junction. The arrows indicate the direction of the electron tunneling and the generated electric field. In the CSISJ, the charges are screened within the range of the charge screening length as indicated by the horizontal dotted lines, while in IJJ's the whole superconducting layer is charged due to the incomplete screening within the single superconducting layer. Consequently, the electric field generated in a junction site penetrates into the neighboring junction sites as the dotted arrows.

Here, let us give a proper Lagrangian, which describes the above DBCN in IJJ's,

$$L_{LD} = \sum_{\ell} \left\{ \frac{s}{8\pi\mu^2} \left(A_0(z_{\ell}, t) + \frac{\hbar}{e^*} \partial_t \theta_{\ell} \right)^2 - \frac{\hbar}{e^*} j_c \left(1 - \cos P_{\ell+1, \ell} \right) + \frac{\epsilon D}{8\pi} E_{\ell+1, \ell}^2 \right\}, \quad (1)$$

where s and D , respectively, are thickness of the superconducting and insulating layer, μ is the charge screening length, ϵ is the dielectric constant, $E_{\ell+1, \ell}$ is the electric field (\perp layers) between $(\ell + 1)$ th and ℓ th superconducting layer, $e^* = 2e$, and $P_{\ell+1, \ell} (\equiv \theta_{\ell+1}(t) - \theta_{\ell}(t) - \frac{\epsilon^*}{\hbar c} \int_{\ell D}^{(\ell+1)D} dz A_z(z, t))$ is the gauge invariant phase difference. In eq.(1) the charge density of ℓ -th superconducting layer, $\rho_{\ell}(t)$, is related to the scalar potential as $\rho_{\ell}(t) = -\frac{1}{4\pi\mu^2} (A_0(z_{\ell}) + \frac{\hbar}{e^*} \partial_t \theta_{\ell})$ in the gauge-invariant form. This Lagrangian corresponds to a discrete version of the well-known time-dependent Ginzburg-Landau theory at $T = 0K$ [10] [11] for stacked multi-Josephson-junction systems when parameters μ and j_c are taken as $\mu = \sqrt{m^* v_f^2 / (12\pi e^* \Delta^2)}$ and $j_c = \hbar e^* \Delta^2 / (MD^2)$, where v_f is the Fermi velocity, Δ is the amplitude of the order parameter at $T = 0K$, and m^* and M are the effective masses parallel and perpendicular to the layers, respectively. The first term in eq.(1) represents the interaction between the charge density and the gauge invariant scalar potential. In conventional theories for CSISJ systems, this term is dropped and the dynamics originating

from only the 2nd and 3rd terms in eq.(1) has so far been intensively studied [11], [12]. This is because the coefficient s/μ^2 is considered to be very large in CSISJ systems and, thus, \mathcal{L} is assumed to have a deep minimum at $\partial_t \theta_{\ell} = -(e^*/\hbar) A_0(z_{\ell})$, which leads to the Josephson relation. Thus, the deviations around this minimum do not give low energy excitations and the Josephson relation always holds within the low energy fluctuations in terms of the phase dynamics in such the CSISJ systems [12]. However, this is not the case in HTSC's, since the thickness, s , of the double superconducting CuO_2 planes is comparable with μ . This means that the fluctuations arising from the first term in eq.(1) cannot be neglected in HTSC's, that is, the energy scale of the charge fluctuations inside the superconducting layers along the c -axis is comparable with that of the AC Josephson effect in HTSC's. This is the essential point which discriminates the IJE's from the AC Josephson effects in conventional serial Josephson-junction arrays.

Let us now prove that the system described by the Lagrangian (1) has the longitudinal plasma mode. To study the response to a longitudinal electric field along the c -axis, we derive the dielectric function in the present system. As is well known, in charged systems the Goldstone mode is absorbed into the longitudinal gauge field and the gauge field becomes massive (the Anderson-Higgs mechanism). In order to describe this situation correctly, it is convenient to utilize the phason gauge proposed by Matsumoto and Umezawa [13], in which the gauge condition is given by $\partial_t A_0(z_{\ell}) + \frac{v_B^2}{c} \frac{A_{\ell+1, \ell}^z - A_{\ell+1, \ell}^z}{D} = 0$, where $A_{\ell+1, \ell}^z \equiv \int_{\ell D}^{(\ell+1)D} dz A_z(z) / D$, and v_B is the velocity of the phason mode and is given by $\sqrt{\frac{8\pi\mu^2}{s} (\frac{e^*}{\hbar})^2 \frac{\hbar}{2e^*} j_c D}$. Here, note that the neutral version of Lagrangian (1), in which dynamics of the gauge field $A_0(z_{\ell})$ and $A_{\ell+1, \ell}^z$ are dropped, gives the Euler equation for θ_{ℓ} in the linear approximation as $[-\partial_t^2 + v_B^2 \frac{1}{D^2} \Delta^{(2)}] \theta_{\ell} = 0$, where $\Delta^{(2)}$ is defined as $\Delta^{(2)} \theta_{\ell} \equiv \theta_{\ell+1} - 2\theta_{\ell} + \theta_{\ell-1}$. For the gauge transformation, $A_{\ell+1, \ell}^z \rightarrow A_{\ell+1, \ell}^z + (\hbar c / e^* D) (\chi_{\ell+1} - \chi_{\ell})$, $A_0(z_{\ell}) \rightarrow A_0(z_{\ell}) - (\hbar / e^*) \partial_t \chi_{\ell}$, the phason gauge condition imposes the equation for χ_{ℓ} , $[-\partial_t^2 + v_B^2 \frac{1}{D^2} \Delta^{(2)}] \chi_{\ell} = 0$, which is the same as the Euler equation for θ_{ℓ} in the neutral case. This result implies that the phason mode can be eliminated by the gauge transformation in the phason gauge, and the Lagrangian (1) is rewritten in the phason gauge as follows,

$$\mathcal{L} = \sum_{\ell} \left\{ \frac{s}{8\pi\mu^2} (A_0(z_{\ell}))^2 - \frac{\hbar}{e^*} j_c \left(1 - \cos \frac{e^* D}{\hbar c} A_{\ell+1, \ell}^z \right) + \frac{\epsilon D}{8\pi} E_{\ell+1, \ell}^2 \right\}. \quad (2)$$

Variation of A_0 for eq.(2) yields one of the Maxwell equations,

$$E_{\ell+1, \ell} - E_{\ell, \ell-1} = -\frac{s}{\epsilon\mu^2} A_0(z_{\ell}). \quad (3)$$

From the relation (3), $E_{\ell+1,\ell} = -\partial_t A_{\ell+1,\ell}^z/c - [A_0(z_{\ell+1}) - A_0(z_\ell)]/D$, and the phason gauge condition, by eliminating the vector potential, we also have another relation between the electric field and the scalar potential,

$$E_{\ell+1,\ell} - E_{\ell,\ell-1} = \frac{D}{v_B^2} (\partial_t^2 - \frac{v_B^2}{D^2} \Delta^{(2)}) A_0(z_\ell). \quad (4)$$

Then, from eqs.(3) and (4) one finds the dielectric function for the electric field perpendicular to the junctions,

$$\epsilon(\omega, k_z) = 1 - \frac{\omega_{\text{pl}}^2}{\omega^2 - 2\alpha\omega_{\text{pl}}^2[1 - \cos k_z(s+D)]}. \quad (5)$$

In deriving eq.(5) we used the relations, $\frac{s}{\epsilon\mu^2} \frac{v_B^2}{D} = \frac{4\pi e^* D}{\epsilon\lambda_c^2} = \frac{c^2}{\omega_{\text{pl}}^2} = \omega_{\text{pl}}^2$ and $\frac{2v_B^2}{D^2} = \frac{8\pi\mu^2}{s} \frac{e^*}{\hbar} j_c = 2\alpha\omega_{\text{pl}}^2$. As seen in eq.(5), the dielectric function has zero points at $\omega(k_z) = \omega_{\text{pl}}\sqrt{1 + 2\alpha[1 - \cos k_z(s+D)]}$, and the longitudinal plasma mode propagating along the c -axis is found to exist. Here, it should be noted that when the first term in the Lagrangian (1) is dropped the obtained Josephson plasma mode has no dispersion.

Next, let us examine dynamics of the Euler-Lagrange equation for the gauge invariant phase difference $P_{\ell+1,\ell}(t)$ derived from the Lagrangian (1) in order to investigate the resistive states in IJJ's. The equation is given by two Maxwell equations derived from the variation of A_0 and A_z for the Lagrangian and the modified Josephson relation obtained by using the gauge invariant charge density expression, $\partial_t P_{\ell+1,\ell}(t) = \frac{e^*}{\hbar} V_{\ell+1,\ell}(t) - \frac{4\pi\mu^2 e^*}{\hbar} (\rho_{\ell+1}(t) - \rho_\ell(t))$, as follows,

$$\frac{1}{\omega_{\text{pl}}^2} \partial_t^2 P_{\ell+1,\ell}(t) + \sin P_{\ell+1,\ell}(t) + \frac{\beta}{\omega_{\text{pl}}} \partial_t P_{\ell+1,\ell}(t) = \frac{I}{j_c} - \alpha (\sin P_{\ell+2,\ell+1}(t) - 2 \sin P_{\ell+1,\ell}(t) + \sin P_{\ell,\ell-1}(t)), \quad (6)$$

where the transport current I and the dissipative (quasi-particle) current are introduced and those satisfy the current conservation relation, $\frac{4\pi}{c} (j_c \sin \theta_{\ell+1,\ell} + \sigma E_{\ell+1,\ell}) + \frac{\epsilon}{c} \partial_t E_{\ell+1,\ell} = I$. Also, $\omega_{\text{pl}} = \frac{c}{\sqrt{\epsilon\lambda_c}}$ and $\beta = \frac{4\pi\sigma\lambda_c}{\sqrt{\epsilon c}} (\equiv \frac{1}{\sqrt{\beta_c}})$, where β_c is the McCumber parameter, and $\alpha (\equiv \frac{\epsilon\mu^2}{sD})$ gives the coupling between junctions. It is clearly found that the parameter α can not be neglected only in IJJ's due to its definition. This model equation has been phenomenologically given by two of us (T.K. and M.T.) [7], and afterwards, Ch.Preis et al. confirmed that the same equation can be derived in their leading order [14]. Here, note that if the first term of L_{LD} is fixed to be zero, the model equation becomes the RCSJ model [12], i.e., the model equation for independent junctions. Also, it should be noted that when I and β are assumed to be zero the linearized eq. (6) has a plane wave solution with the same dispersion relation as the relation derived from eq.(5) [7], [9]. In order to obtain the MBS, we numerically solve eq.(6) for ten identical junctions under

the periodic boundary condition. The values of parameters in eq.(6) α and β , respectively, are chosen as 0.1 and 0.20, supposing Bi-2212 case. Although in our previous paper [9] α was taken as 2.27, the present value employed was proved to be reasonable in Bi-2212 [14].

Figure 2(I) is a hysteresis loop in I-V curve for eq.(6). In obtaining this curve, the current I is increased first up to a value above the critical current j_c and then decreased to zero along the arrows in Fig.2(I). In the current increasing process, we find a jump at j_c , where all junctions synchronously switch into same resistive states. In Fig.2(II), the time developments of the normalized Josephson currents $\sin P_{\ell+1,\ell}$ at the point B are plotted for all junction sites. As seen in this figure, all junctions show a synchronous whirling motion. In decreasing the current from the point B, we find several step-like structures as seen in Fig.2(I). Figure 2(III) and (IV) show the time developments of $\sin P_{\ell+1,\ell}$ of all junction sites at the point C and D, respectively. It is found that some junctions are in the resistive state, in which $\sin P_{\ell+1,\ell}$ periodically varies from -1 to 1, while the others are in the superconducting state, in which it shows tiny oscillatory motions. By monitoring the time evolution of $\sin P_{\ell+1,\ell}$ in the region around the point C and D as Fig.2(III) and (IV), one may see that in decreasing the current the number of the resistive junctions decreases together with the step-like structures as seen in Fig.2(III) and (IV). Such the behaviors are never observed in the case without the coupling, i.e., $\alpha = 0$ in eq.(6), which shows only a switching behavior into the superconducting state of all resistive junctions at a constant current value.

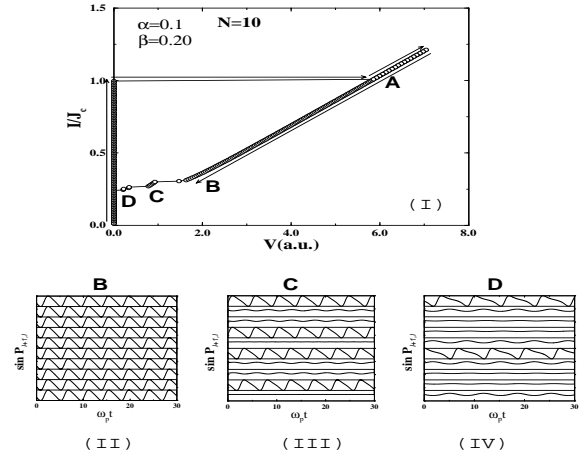


FIG.2 (I) The I-V hysteresis curve obtained by the current increasing and decreasing along the arrows. The time developments of $\sin P_{\ell+1,\ell}$ of all junctions from $\ell = 0$ to $\ell = 9$ at (II) the point B, (III) the point C, and (IV) the point D in the I-V hysteresis curve (I).

Let us now study the region around the point C and D in more details. In Fig.3(a), we present the I-V curve enlarged in the region around C and D. In this region,

we can get different I-V curves when intervals δI of the decrease in the current value is changed. In the Fig.3(a), two cases with different δI are plotted. Those behaviors imply that several bifurcation points are distributed in a very narrow region for the controlling parameter I of eq.(6). This is a contrast to the case of $\alpha = 0$. Thus, in order to obtain all possible branches in trajectories of eq.(6) in the current decreasing process, we perform the calculations many times, changing the decreasing current interval δI . Then, when the current is reincreased from suitable points of the obtained branches along the arrows as seen in Fig.3(a), we can obtain several I-V branches, which finally lead to the MBS as shown in Fig.3(b). The simulated MBS is composed of equidistant branches and the number of resistive branches (=10) is equal to the number of junctions (=10). However, in the present simulation, it should be noted that we introduce Nyquist noise to get the first and ninth branches. But, after the transitions by the introduction of the noise, those two branches could be stably traced without the noise in the current reincreasing.

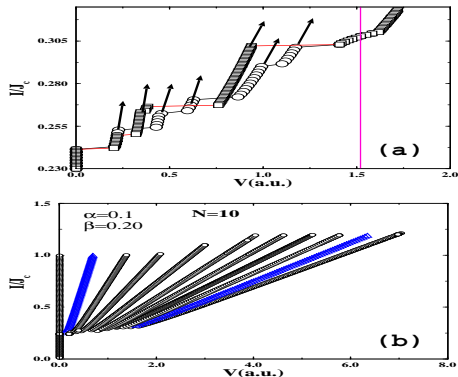


FIG.3 (a) The enlarged view of the transition region in I-V curve. The circles and square points show different I-V curves obtained by changing the interval of the decrease in the current value. (b) The MBS in the I-V curve obtained by the current reincreasing process along the arrows as indicated in (a).

Thus, all the resistive branches can be understood to correspond to stable trajectories in the phase space of eq.(6), and the MBS as observed in Bi-2212 SC's can be reproduced by eq.(6) without inhomogeneities of junction parameters. In addition, we mention that if a free boundary condition, in which the top and bottom junctions are distinguished from internal ones, is employed, we can obtain all the branches without any noise. In the actual experiments for the MBS, the current decreasing and increasing are performed many times. The present simulations also require a number of careful current decreasing and increasing process.

Finally, let us consider why eq.(6) can give MBS's as observed in Bi-2212. The question resolves itself into the following two points. The first one is why several step-

like transitions occur in decreasing the current as seen in Fig.3(a) and the second one is why those branches can keep their stabilities in the current reincreasing process as seen in Fig.3(b). In this paper, we focus on only the first point. This is because Takeno et al. have already touched the second point in a context for stabilities of localized whirling (rotating) motions in the different coupled rotator models with the coupling given by trigonometric functions [15] and they proved that the bounded character of the trigonometric function is essential for the existence of the localized rotating motions [15]. As shown before, we observe that those step-like jumps in the current decreasing result from the step-wise transitions of resistive junctions into the superconducting state as seen in Fig.2(III) and (IV). This implies that although all junctions are identical each junction can switch into the superconducting state at a different current value I/j_c . These behaviors closely resemble those of the independent RCSJ model under the presence of inhomogeneous distributions in junction parameters. We easily notice from the right hand side of eq.(6) that the total driving force (current) acting on a junction can be classified into two components, which are the normalized external current I/j_c and the normalized Josephson current in neighboring junctions, $I_{nbj} = -\alpha(\sin P_{\ell+2,\ell+1}(t) + \sin P_{\ell,\ell-1}(t))$, where the term $2\alpha \sin P_{\ell+1,\ell}$ is transposed to the left hand side. Thus, it is clearly found that the total driving force acting on each junction depends on the dynamical state of neighboring junctions. Here, in order to demonstrate it, let us suppose that ℓ -th junction is the resistive state and consider two simple cases, in which both of the neighboring ($\ell \pm 1$)-th junctions are in the superconducting state and both are in the resistive one. In the former case, since the neighboring junctions show only the tiny oscillations around the stable points, I_{nbj} is very small ($I_{nbj} \sim 0$), and the total driving current almost equal to the external current I/j_c . On the other hands, in the latter case, the minimum of the instantaneous driving current is given by $I/j_c - 2\alpha$, and it can sufficiently become smaller than that of the former case. This clearly implies that in the current decreasing process the superconducting transition of ℓ -th junction in the latter case occurs prior to the former case. Thus, it is found that the switching current value of each junction is dependent on dynamical states of neighboring junctions and therefore the superconducting transition points in eq.(6) are distributed in the range of the controlling parameter I . From those considerations, it is found that the origin of the dynamical transitions between branches is the coupling between junctions due to the charge incomplete screening within the single superconducting layer, i.e., the DBCN inside the superconducting layer.

In conclusion, we show that the DBCN inside the superconducting layer is essential for atomic-scale stacked Josephson junction systems as IJJ's, and give the proper model Lagrangian for IJJ's describing the DBCN. We clarify that the Lagrangian involves the dynamics of the lon-

itudinal propagating Josephson plasma responsible for the MRA observed in the longitudinal configuration while the Euler-Lagrange equation under the transport and the dissipative current can reproduce the MBS.

The authors thank C.Helm and H.Matsumoto for illuminating discussions and one of us (M.M.) also thank A.Tanaka for useful discussions and K. Asai and H. Kaburaki for their supports on the computer simulations in JAERI.

-
- [1] M.Tachiki, T.Koyama, and S.Takahashi, *Phys.Rev.* **B50**, 7065(1994).
- [2] L.N.Bulaevskii, M.P.Maley, and M.Tachiki, *Phys.Rev.Lett.* **74**, 801(1995).
- [3] Y. Matsuda, M. B. Gaifullin, K. Kumagai, K. Kadowaki, and T. Mochiku, *Phys. Rev. Lett.* **75**, 4512 (1995).
- [4] R.Kleiner, F.Steinmeyer, G.Kunkel, and P.Müller, *Phys.Rev.Lett.* **68**, 2394(1992).
- [5] I.Keepa et al. *Phys.Rev.* **B57**,3108(1998).
- [6] M.Tachiki, T.Koyama, and S.Takahashi, in *Coherence in High Temperature Superconductors*, edited by G.Deutcher and A.Revcolevshi (World Scientific Singapore, 1996), p.371;
- [7] T.Koyama and M.Tachiki, *Phys.Rev.* **B54**, 16183(1996).
- [8] K.Schlenga et al., *Phys.Rev.* **57**, 14518(1998), and many references therein.
- [9] M.Machida, T.Koyama, and M.Tachiki, *Physica C* **300** 55(1998).
- [10] M.J.Stephen and H.Suhl, *Phys.Rev.* **13**,797(1964); E.Abraham and T.Tsuneto, *Phys.Rev.* **152**, 416(1966)
- [11] E.Šimánek, *Inhomogeneous Superconductors* (Oxford, 1994), and many reference therein.
- [12] V.Ambegaokar, U.Eckern, and G.Schon, *Phys. Rev. Lett.***48**, 1745(1982); U.Eckern, G.Schon, and V.Ambegaokar *Phys. Rev.***B30**, 6419(1984).
- [13] H.Matsumoto and H.Umezawa, *Fortshritte der physik* 24,357(1976); H.Umezawa, H.Matsumoto, and M.Tachiki, *Thermo Field Dynamics and Condensed States* (North-Holland, 1982).
- [14] Ch.Preis, Ch.Helm, J.Keller, A.Sergeev, and R.Kleiner, *SPIE Conference Proceedings "Superconducting Superlattices II"*, 236(1998).
- [15] S.Takeno, and M.Peyard, *Physica D* **92**, 140(1996); see also Z.Zheng, B.Hu, and G.Hu, *Phys. Rev.* **E57**,1139(1998).